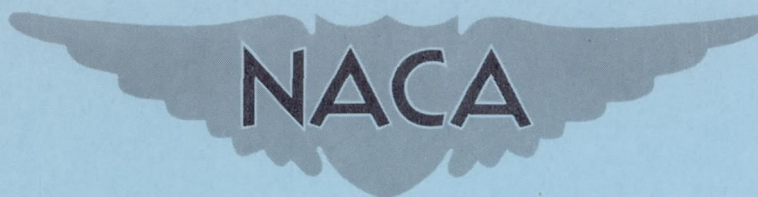


RM A52E23

NACA RM A52E23



# RESEARCH MEMORANDUM

EFFECTS OF SIMULATED SKIN WRINKLES OF THE WING SURFACE ON THE  
AERODYNAMIC CHARACTERISTICS OF TWO WING-BODY COMBINATIONS  
EMPLOYING WINGS OF LOW ASPECT RATIO AT  
SUBSONIC AND SUPERSONIC SPEEDS

By John C. Heitmeyer and Willard G. Smith

Ames Aeronautical Laboratory  
Moffett Field, Calif.

NATIONAL ADVISORY COMMITTEE  
FOR AERONAUTICS  
WASHINGTON

August 5, 1952  
Declassified September 1, 1959



## NATIONAL ADVISORY COMMITTEE FOR AERONAUTICS

RESEARCH MEMORANDUM

EFFECTS OF SIMULATED SKIN WRINKLES OF THE WING SURFACE ON THE  
AERODYNAMIC CHARACTERISTICS OF TWO WING-BODY COMBINATIONS  
EMPLOYING WINGS OF LOW ASPECT RATIO AT  
SUBSONIC AND SUPERSONIC SPEEDS

By John C. Heitmeyer and Willard G. Smith

## SUMMARY

This report is concerned with the results of an investigation to determine the effects of simulated skin wrinkling of the wing surfaces on the aerodynamic characteristics of two wing-body combinations.

The lift, drag, and pitching moment of a low-wing wing-body combination employing a plane triangular wing of aspect ratio 3 with and without simulated skin wrinkles on the upper surface of the wing are presented for a range of Mach numbers from 0.60 to 0.92 and from 1.20 to 1.90 at a Reynolds number of 4.8 million.<sup>1</sup>

The lift, drag, and pitching moment of a midwing interceptor model incorporating a plane swept wing of aspect ratio 2 with and without skin wrinkles on the lower surface of the wing are presented for a range of Mach numbers from 0.60 to 0.90 and from 1.20 to 1.70. In addition, the variation of the hinge-moment coefficient with angle of attack of two elevon control surfaces on the swept-wing model is presented for a Mach number of 0.90. All data for this wing were obtained at a constant Reynolds number of 2.0 million.

## INTRODUCTION

It is well known that airplane wings when subjected to loadings such as encountered in gust and high-speed maneuvers exhibit surface wrinkling. To determine the effect of these surface irregularities on the aerodynamic characteristics of wing plan forms suitable for high-speed flight, tests

---

<sup>1</sup>At a Mach number of 1.90, wind-tunnel power limited the maximum test Reynolds number to 3.1 million.

---

have been made at subsonic and supersonic Mach numbers of two wing-body combinations each with and without simulated skin wrinkles on the wing surface. A low-wing model employing a plane triangular wing of aspect ratio 3 and a midwing model of an interceptor airplane employing a plane swept wing of aspect ratio 2 were selected for investigation, since experimentally determined data on the shape and distribution of wrinkles were available from static loading tests of a full-scale airplane similar to the triangular-wing model and from static loading tests of a prototype airplane of the interceptor model.

## NOTATION

$b$	wing span
$\bar{c}$	mean aerodynamic chord $\left( \frac{\int_0^{b/2} c^2 dy}{\int_0^{b/2} c dy} \right)$
$c$	local wing chord
$\frac{L}{D}$	lift-drag ratio
$\left( \frac{L}{D} \right)_{\max}$	maximum lift-drag ratio
$M$	Mach number
$M_a$	first moment of area of elevon surface about hinge line (area ahead of hinge line excluded)
$q$	free-stream dynamic pressure
$R$	Reynolds number based on the mean aerodynamic chord
$S$	total wing area including area formed by extending leading and trailing edges to plane of symmetry
$C_D$	drag coefficient $\left( \frac{\text{drag}}{qS} \right)$
$C_L$	lift coefficient $\left( \frac{\text{lift}}{qS} \right)$
$C_h$	hinge-moment coefficient $\left( \frac{\text{hinge moment}}{2qM_a} \right)$



- $C_m$       pitching-moment coefficient about a horizontal axis through the point on the body axis at the body station corresponding to the quarter point of the mean aerodynamic chord
- $$\left( \frac{\text{pitching moment}}{qS\bar{c}} \right)$$
- $\alpha$       angle of attack of body axis, degrees
- $\delta$       angle between wing chord and elevon chord, measured in a plane perpendicular to the elevon hinge line, positive for downward deflection, degrees

#### Subscripts

- i      inboard elevon
- o      outboard elevon

#### APPARATUS

##### Model

Wrinkle description.— The crest-to-crest distance, amplitude, and location of the skin wrinkles on the upper surface of the triangular-wing model (see fig. 1) were scaled from corresponding experimental values obtained from a 5 g static loading of a full-scale low-wing airplane employing a nearly triangular wing with  $55^\circ$  swept leading edges. These static loading tests represented five times the loading which the wing would encounter in unaccelerated level flight at a Mach number of 0.90 at an altitude of 10,000 feet with a 33 pounds per square foot wing loading.

The wrinkle pattern (see fig. 2) which was simulated on the lower surface of the swept-wing model was scaled from a wrinkle pattern observed during static loading tests of a prototype airplane. This loading corresponded to a 7 g acceleration of an airplane having a wing loading of 50 pounds per square foot, and flying at a Mach number of 0.90 at an altitude of 10,000 feet. The wrinkles appeared on the lower surface of the wing, because the elevon download (upward elevon deflection) necessary for balance at the high lift coefficients is transmitted as a compression load into the region ahead of the hinge line on the lower surface of the wing. To simulate the flight condition at which the wrinkles occurred the model was tested with both elevon control surfaces deflected  $15^\circ$  upward.



The cross-sectional shape of the wrinkles simulated on each model was a circular arc. The crest-to-crest distance, amplitude, and location of the wrinkles on the triangular-wing model and on the swept-wing model are shown in figures 3 and 4, respectively. The wrinkled surface of each model was simulated by coating the wings of the basic models with wax from which the desired wrinkle pattern was cut by means of scrapers contoured to the desired cross section.

Basic models.— The important geometric characteristics of the models investigated are as follows:

Wing	Triangular-wing model	Swept-wing model
Aspect ratio . . . . .	3	2
Taper ratio . . . . .	0	0.332
Airfoil section (streamwise).	NACA 0003-63	Root, NACA 0007-63/30-9.5° Tip, NACA 0004.5-63/30-9.5°
Total area, square feet . .	2.425	1.680
Mean aerodynamic chord, feet.	1.199	1.003
Dihedral, degrees . . . . .	0	0
Camber . . . . .	None	None
Twist, degrees . . . . .	0	0
Incidence, degrees . . . . .	0	0
Distance, wing chord plane to body axis, percent of $\bar{c}$ . . . . .	13.7	0
Control surfaces		
First moment of area of inboard elevon, $M_{a_i}$ . . .	None	0.00147
First moment of area of outboard elevon, $M_{a_o}$ . . .	None	0.00222



## Wind Tunnel and Equipment

The experimental investigation was conducted in the Ames 6- by 6-foot supersonic wind tunnel. In this tunnel, the Mach number can be varied continuously and the stagnation pressure can be regulated to maintain a given test Reynolds number. The air is dried to prevent formation of condensation shocks. Further information on this tunnel is presented in reference 1.

The models were sting mounted in the tunnel with the pitch plane horizontal. The diameter of the straight sting used to mount the triangular-wing model was about 93 percent of the diameter of the body base. A sting bent  $5^\circ$  in the direction of positive lift was used to mount the swept-wing model, the diameter of the sting being about 64 percent of the diameter of the body base. Due to the bend in the sting, the swept-wing model was displaced laterally about 4 inches from the tunnel center line. The 4-inch-diameter, four-component, strain-gage balance, which was enclosed within the body of the triangular-wing model, is described in reference 2. The 2-1/2-inch-diameter, three-component, strain-gage balance, which was enclosed within the body of the swept-wing model, is of the same type as that described in reference 2.

## TESTS AND PROCEDURE

### Range of Test Variables

The lift, drag, and pitching moment of the triangular-wing model were investigated for a range of Mach numbers from 0.60 to 0.92, and from 1.20 to 1.90. The data were obtained at a constant Reynolds number of 4.8 million for all Mach numbers except 1.90. At this Mach number, wind-tunnel power limited the test Reynolds number to 3.1 million. The lift, drag, and pitching moment of the swept-wing model were investigated for a range of Mach numbers from 0.60 to 0.90 and from 1.20 to 1.70. The hinge-moment characteristics of two control surfaces were also obtained on the swept-wing model at a Mach number of 0.90. The data for the swept-wing model were obtained at a constant Reynolds number of 2.0 million.

### Reduction of Data

The test data have been reduced to standard coefficient form. Factors which could affect the accuracy of these results, together with the corrections applied, are discussed in the following paragraphs.



Tunnel-wall interference.— Corrections to the subsonic results for the induced effects of the tunnel walls resulting from lift on the model were made according to the methods of reference 3. The numerical values of these corrections (which were added to the uncorrected data) for each model were obtained from:

Triangular-wing model

$$\Delta\alpha = 0.554 C_L$$

$$\Delta C_D = 0.0097 C_L^2$$

Swept-wing model

$$\Delta\alpha = 0.377 C_L$$

$$\Delta C_D = 0.0066 C_L^2$$

No corrections were made to the pitching-moment coefficients.

The effects of constriction of the flow at subsonic speeds by the tunnel walls were taken into account by the method of reference 4. This correction was calculated for conditions at zero angle of attack and was applied throughout the angle-of-attack range. For the triangular-wing model at a Mach number of 0.90 this correction amounted to a 2-percent increase in the Mach number and in the dynamic pressure over that determined from a calibration of the wind tunnel without a model in place. This correction, at a Mach number of 0.90, amounted to only a 1-percent increase in the Mach number and in the dynamic pressure for the swept-wing model.

During the tests at supersonic speeds, the reflection from the tunnel walls of the Mach wave originating at the nose of the body did not cross the model. No corrections were required, therefore, for tunnel-wall effects.

Stream variations.— No tests have been made at subsonic and supersonic speeds of the triangular-wing model in both the normal and inverted positions for the purposes of determining stream inclination and stream curvature. However, results of similar tests of a midwing model (reference 5) employing the same wing as the present triangular-wing model have indicated at subsonic speeds a stream inclination of  $-0.05^\circ$  and a stream curvature capable of producing a pitching-moment coefficient of  $-0.004$  at zero lift, and no stream inclination or stream curvature at supersonic speeds. Tests of the swept-wing model in both the normal and inverted positions at subsonic and supersonic Mach numbers have indicated a stream inclination of less than  $-0.10^\circ$  at subsonic speeds, and neither stream inclination nor stream curvature at supersonic speeds. No corrections were made to the data of either model for the effects of the stream irregularities at subsonic speeds.

No measurements have been made to determine the stream curvature in the yaw plane of the models at subsonic speeds. A survey of the air stream



(reference 1) at supersonic speeds has shown a stream curvature in the yaw plane of the models. The effects of this curvature on the measured characteristics of the present models are not known but are believed to be small, as judged by the results of reference 6.

At subsonic speeds, the longitudinal variation of static pressure in the region of the models is not known accurately at present, but a preliminary survey has indicated that it is less than 2 percent of the dynamic pressure. No correction for this effect was made. The survey of reference 1 indicated that at supersonic speeds there is a static pressure variation in the test section of sufficient magnitude to affect the drag results. A correction,  $\Delta C_{DG}$ , was added to the measured drag coefficient, therefore, to account for the longitudinal buoyancy caused by this static pressure variation. These corrections are as follows:

Triangular-wing model	
M	$\Delta C_{DG}$
1.20	0
1.40	-.0003
1.70	.0010
1.90	.0006

Swept-wing model	
M	$\Delta C_{DG}$
1.20	-0.0004
1.35	-.0010
1.50	0
1.70	.0004

Support interference.— At subsonic speeds the effects of support interference on the aerodynamic characteristics of the present models are not known. For these tailless models, it is believed that such effects consisted primarily of a change in the pressure at the base of each model. In an effort to correct at least partially for this support interference, the base pressure was measured and the drag data were adjusted to correspond to a base pressure equal to the static pressure of the free stream.

At supersonic speeds, the effects of support interference on a body-sting configuration similar to that of the present models are shown by reference 7 to be confined to a change in base pressure. The previously mentioned adjustment of the drag for base pressure, therefore, was applied at supersonic speeds. It should be noted that the drag coefficients presented in the present report are in essence foredrag coefficients since the base drag, drag which a model would encounter in free flight, is not included.



## RESULTS

The variation of lift coefficient with angle of attack, and the variation of pitching-moment coefficient, drag coefficient, and lift-drag ratio with lift coefficient for the triangular-wing model and for the swept-wing model are shown in figures 5 and 6, respectively.

The variation of hinge-moment coefficient with angle of attack for the inboard elevon and for the outboard elevon of the swept-wing model is presented in figure 7.

It should be mentioned that the results as presented are for specific wrinkle patterns corresponding to prescribed loadings of given wing structures. For the given wing loading and altitude (lift coefficient of 0.45 at a Mach number of 0.60, lift coefficient of 0.06 at a Mach number of 1.70) the major effect of the skin wrinkles on the characteristics of the triangular-wing model was to increase the drag coefficient and to decrease the lift-drag ratio at all Mach numbers, except at a Mach number of 0.60 where no effect was indicated. The lift and pitching-moment characteristics were unaffected.

For the swept-wing model with the given wing loading and altitude, the balance lift coefficient at all Mach numbers is approximately equal to the lift coefficient required for a 7 g acceleration. The results indicate that at this lift coefficient the wrinkles increased the drag by a small amount at supersonic Mach numbers and had negligible effect on the drag at subsonic Mach numbers. The lift and pitching-moment characteristics at subsonic and supersonic Mach numbers were unaffected. At a Mach number of 0.90 the presence of the simulated skin wrinkles decreased slightly the hinge-moment coefficients of each elevon control surface.

Ames Aeronautical Laboratory  
National Advisory Committee for Aeronautics  
Moffett Field, California

## REFERENCES

1. Frick, Charles W., and Olson, Robert N.: Flow Studies in the Asymmetric Adjustable Nozzle in the Ames 6- by 6-Foot Supersonic Wind Tunnel. NACA RM A9E24, 1949.



2. Olson, Robert N., and Mead, Merrill H.: Aerodynamic Study of a Wing-Fuselage Combination Employing a Wing Swept Back  $63^{\circ}$  - Effectiveness of an Elevon as a Longitudinal Control and the Effects of Camber and Twist on the Maximum Lift-Drag Ratio at Supersonic Speeds. NACA RM A50A31a, 1950.
3. Glauert, H.: Wind-Tunnel Interference on Wings, Bodies, and Airscrews. R.&M. No. 1566, British A.R.C., 1933.
4. Herriot, John G.: Blockage Corrections for Three-Dimensional-Flow Closed-Throat Wind Tunnels, With Consideration of the Effect of Compressibility. NACA Rep. 995, 1950. (Formerly NACA RM A7B28)
5. Heitmeyer, John C.: Lift, Drag, and Pitching Moment of Low-Aspect-Ratio Wings at Subsonic and Supersonic Speeds - Plane Triangular Wing of Aspect Ratio 3 With NACA 0003-63 Section. NACA RM A51H02, 1951.
6. Lessing, Henry C.: Aerodynamic Study of a Wing-Fuselage Combination Employing a Wing Swept Back  $63^{\circ}$  - Effect of Sideslip on Aerodynamic Characteristics at a Mach number of 1.4 With the Wing Twisted and Cambered. NACA RM A50F09, 1950.
7. Perkins, Edward W.: Experimental Investigation of the Effects of Support Interference on the Drag of Bodies of Revolution at a Mach Number of 1.5. NACA TN 2292, 1951.







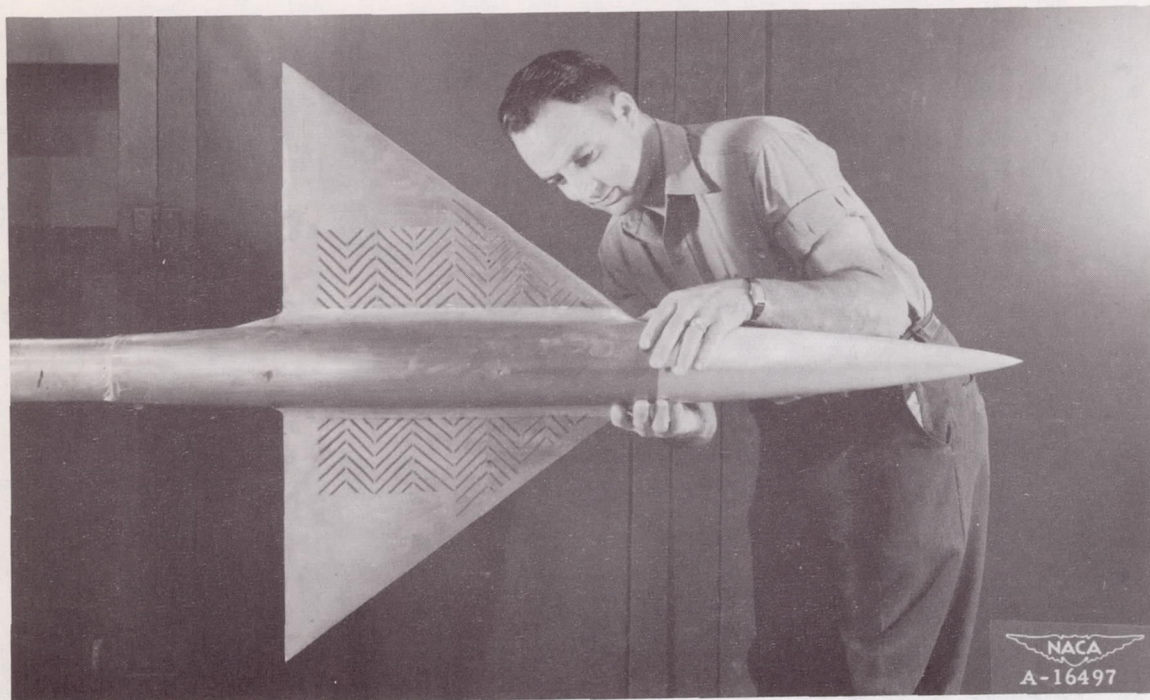


Figure 1.- The triangular-wing model with the simulated skin wrinkles on the upper wing surface.



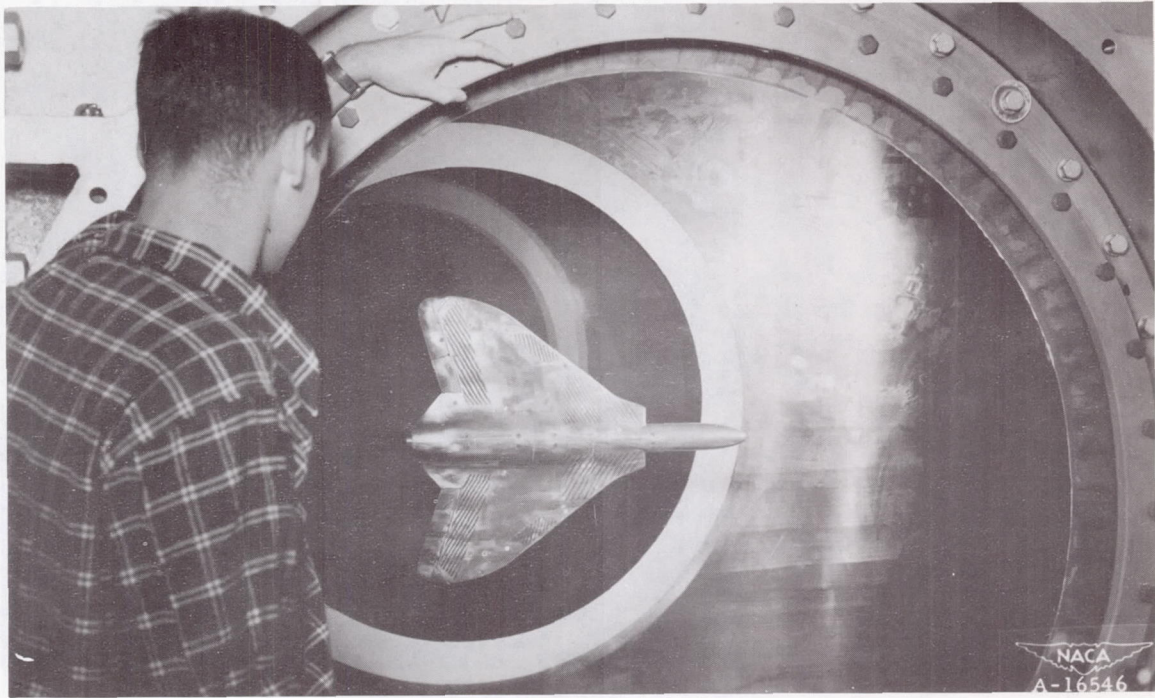


Figure 2.- The swept-wing model with the simulated skin wrinkles on the lower wing surface.

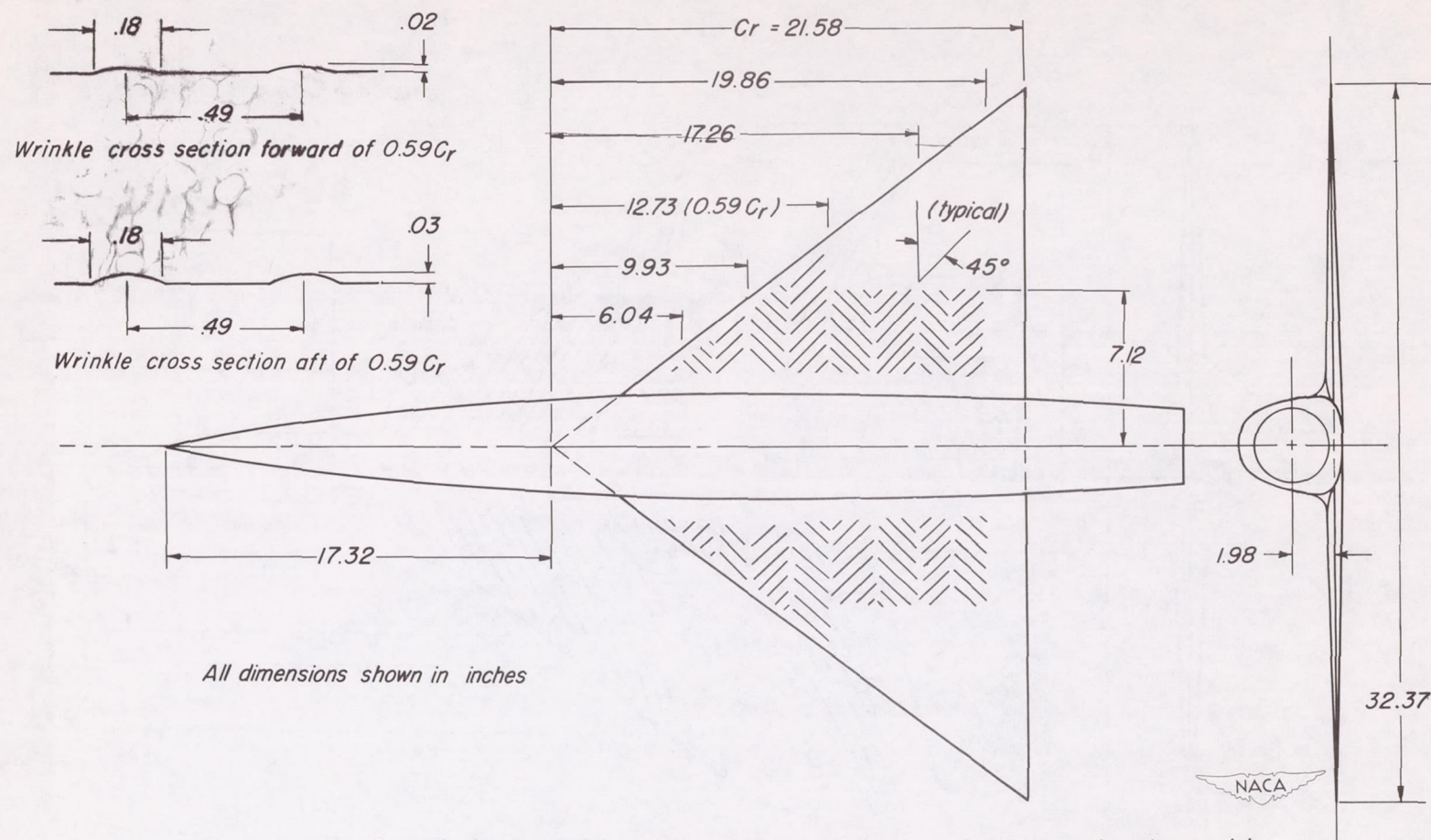


Figure 3. - Location of simulated skin wrinkles on the upper surface of the triangular-wing model.



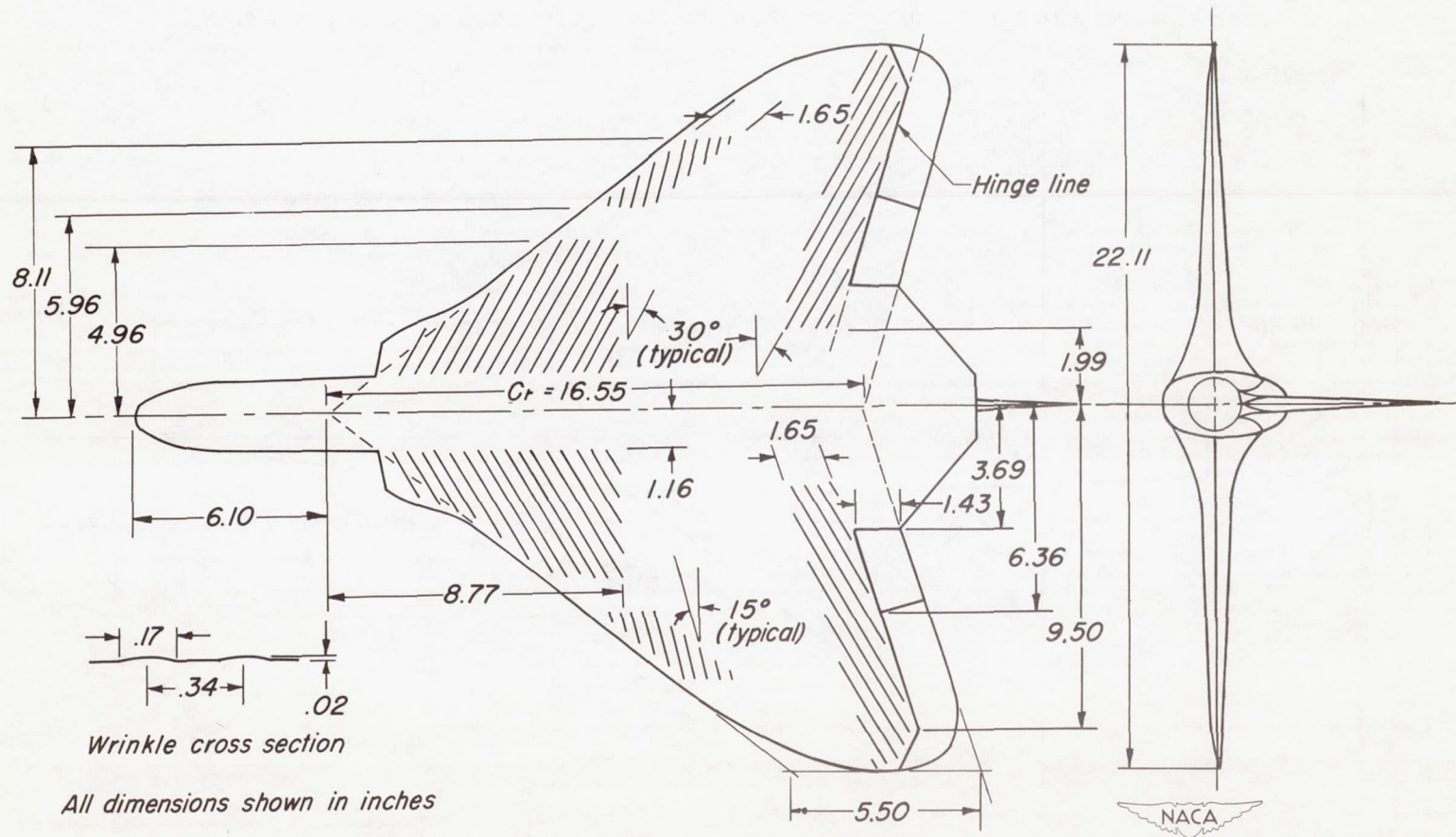
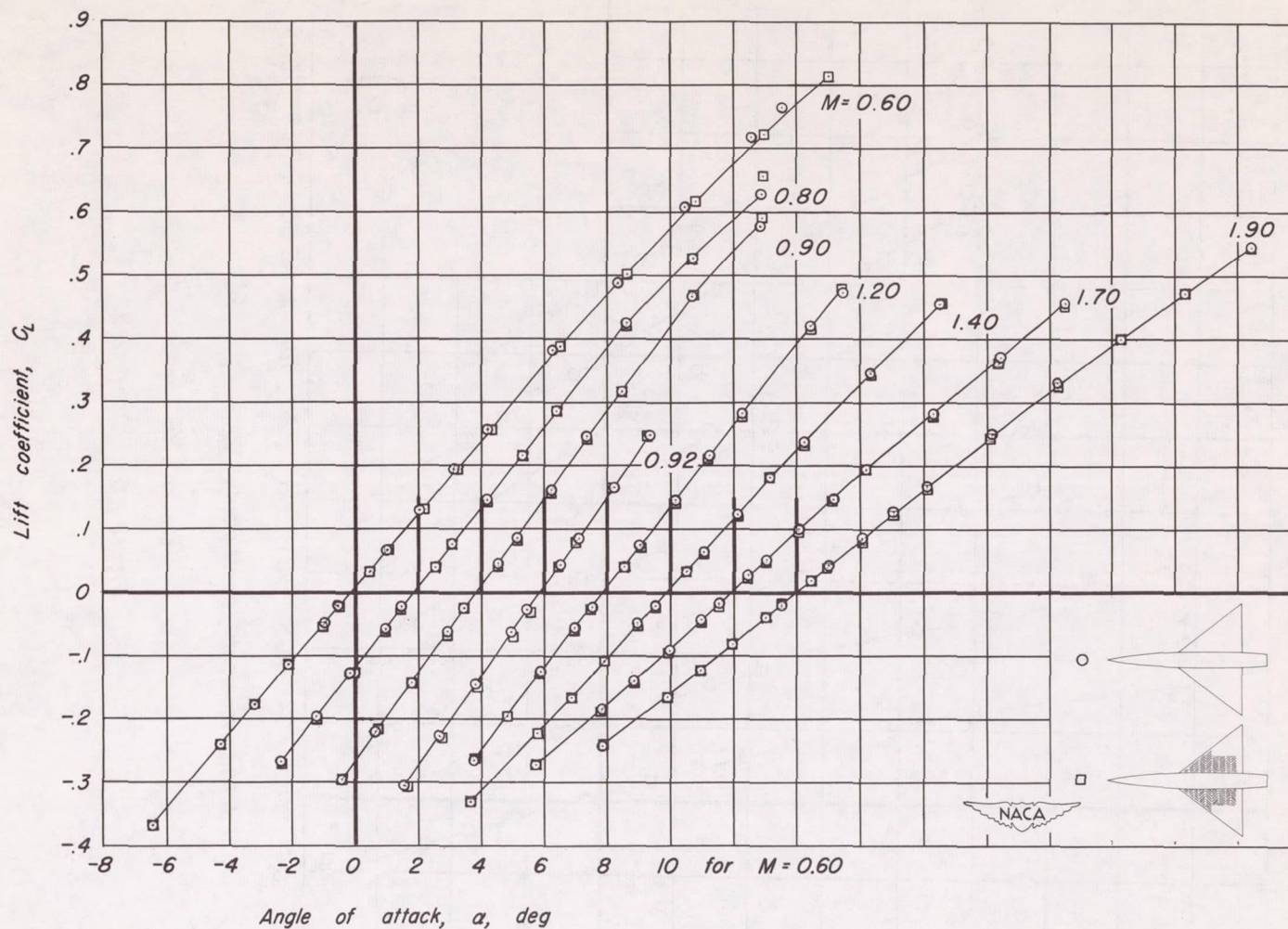


Figure 4. - Location of simulated skin wrinkles on the lower surface of the swept-wing model.



(a)  $C_L$  vs  $\alpha$

Figure 5.- The effect of simulated skin wrinkles on the variation of the aerodynamic characteristics with lift coefficient for the triangular-wing model.



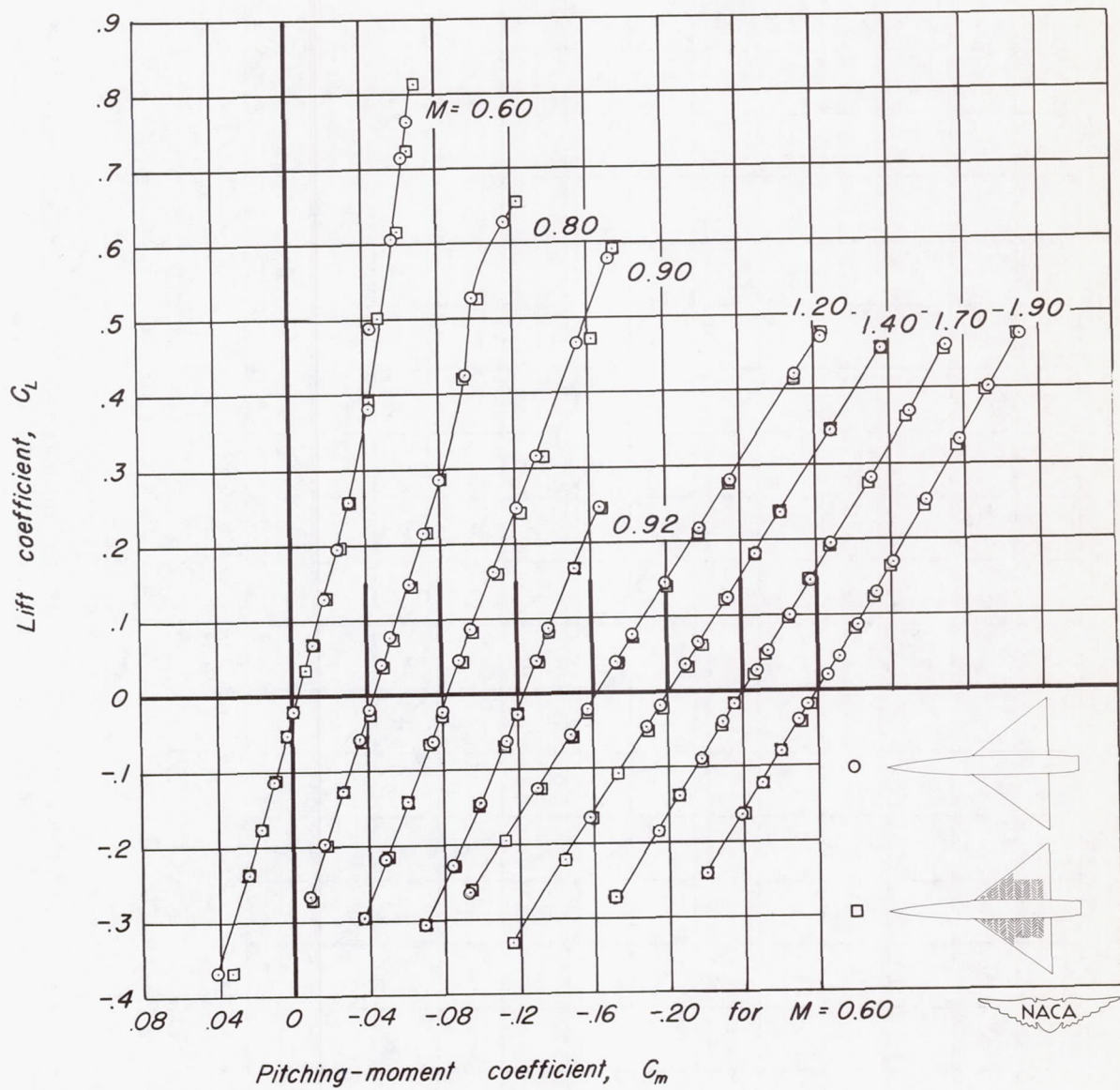
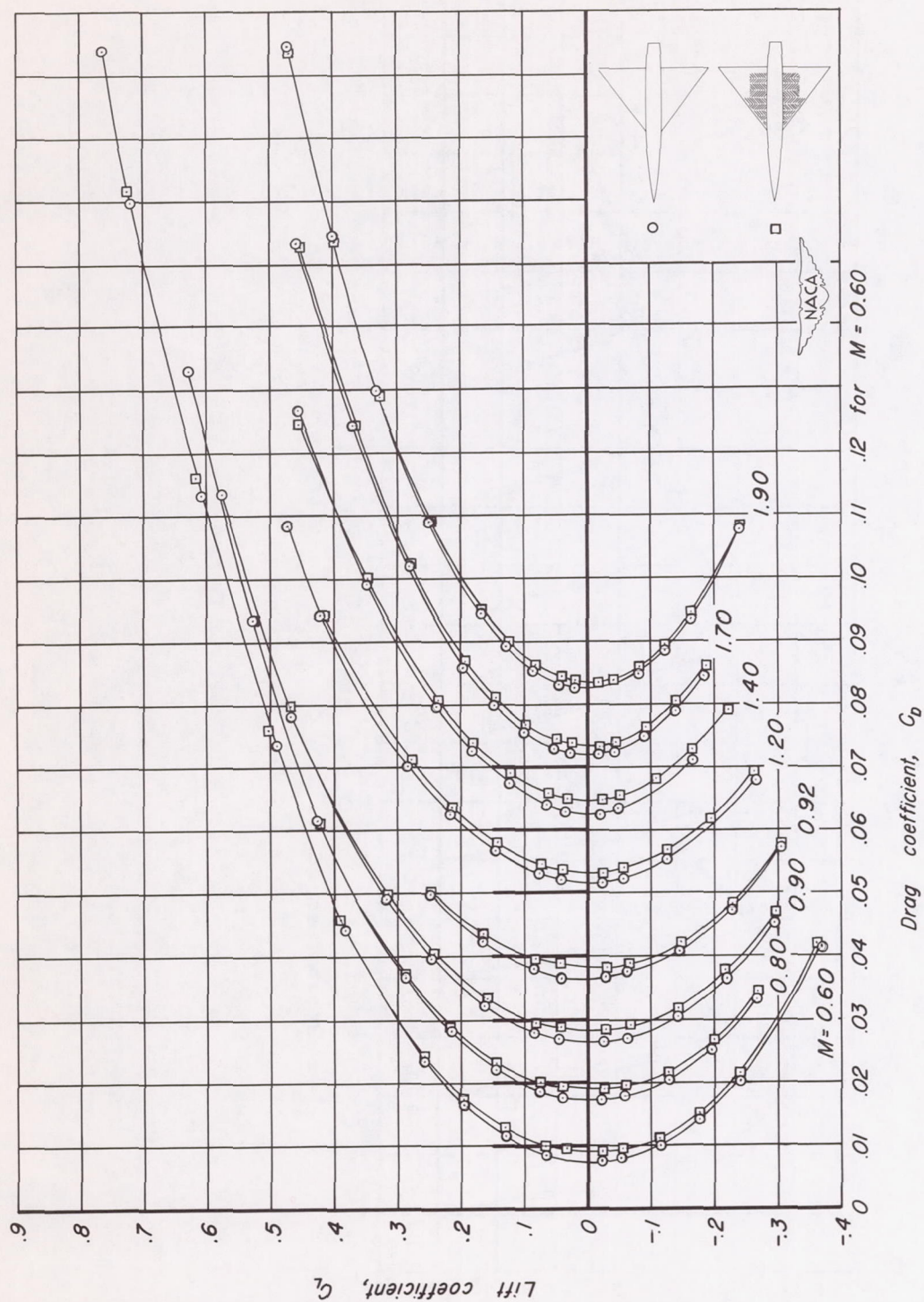
(b)  $C_L$  vs  $C_m$ 

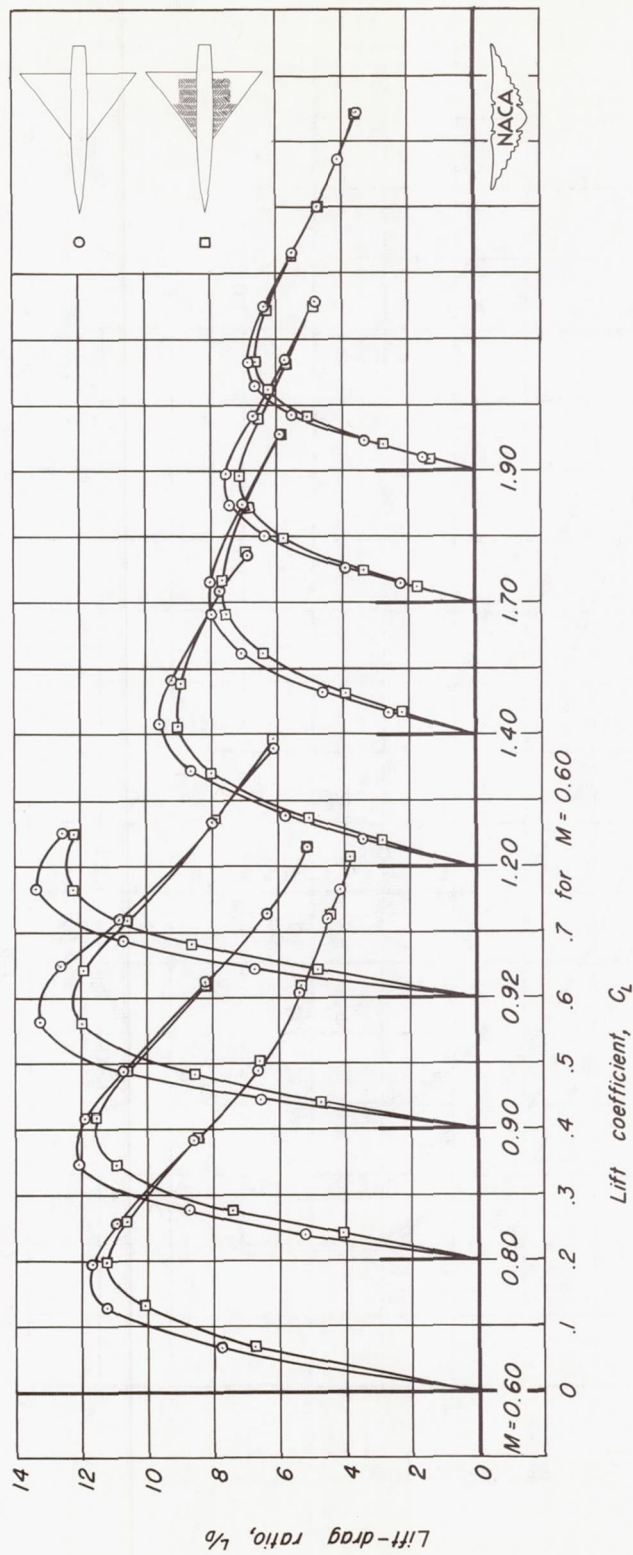
Figure 5. - Continued.



(c)  $C_L$  vs  $C_D$

Figure 5. - Continued.





(d)  $L/D$  vs  $C_L$

Figure 5. - Concluded.

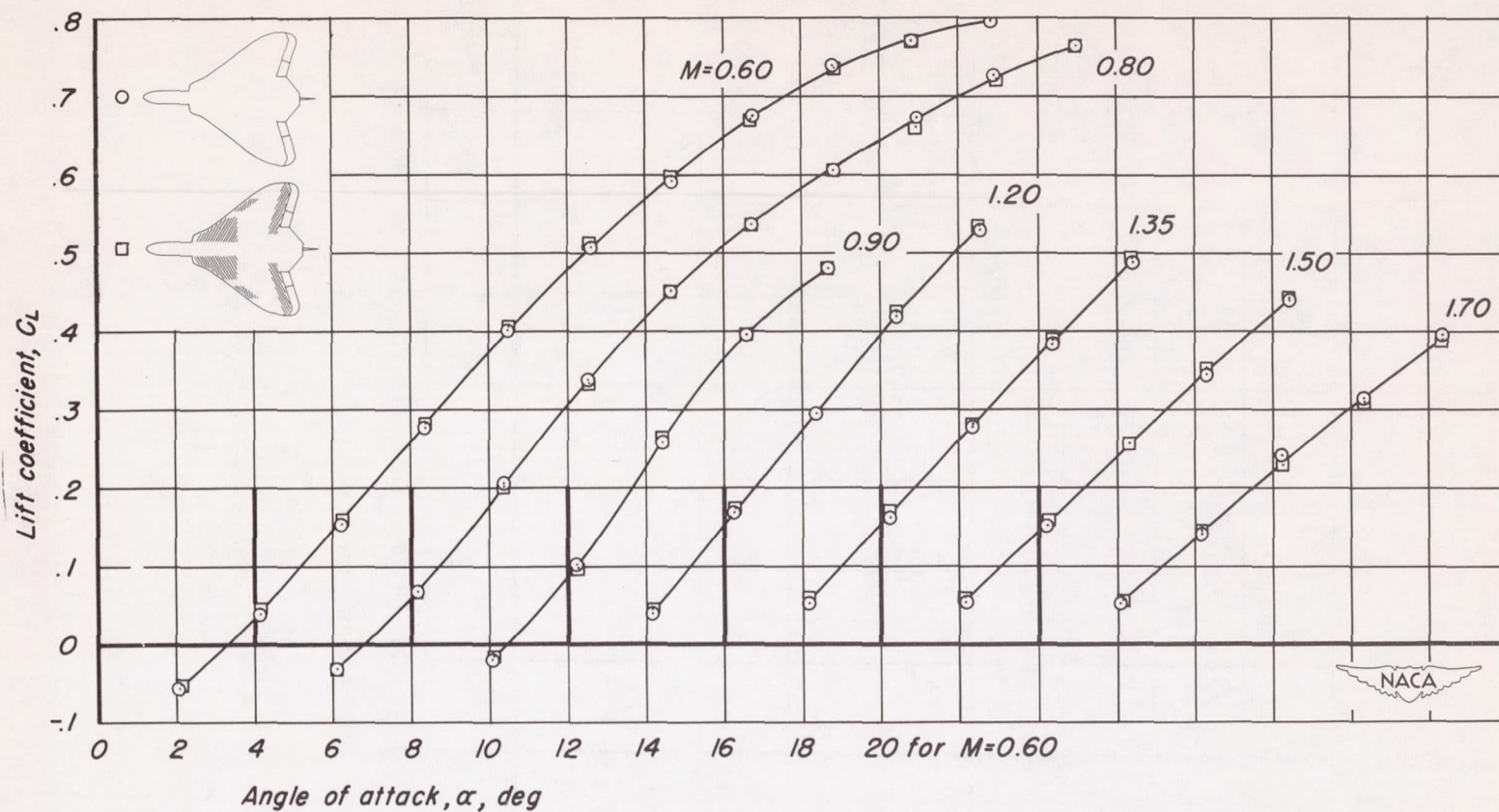
(a)  $C_L$  vs  $\alpha$ 

Figure 6.-The effect of simulated skin wrinkles on the variation of the aerodynamic characteristics with lift coefficient for the swept-wing model.

$\delta_i, -15^\circ; \delta_o, -15^\circ$



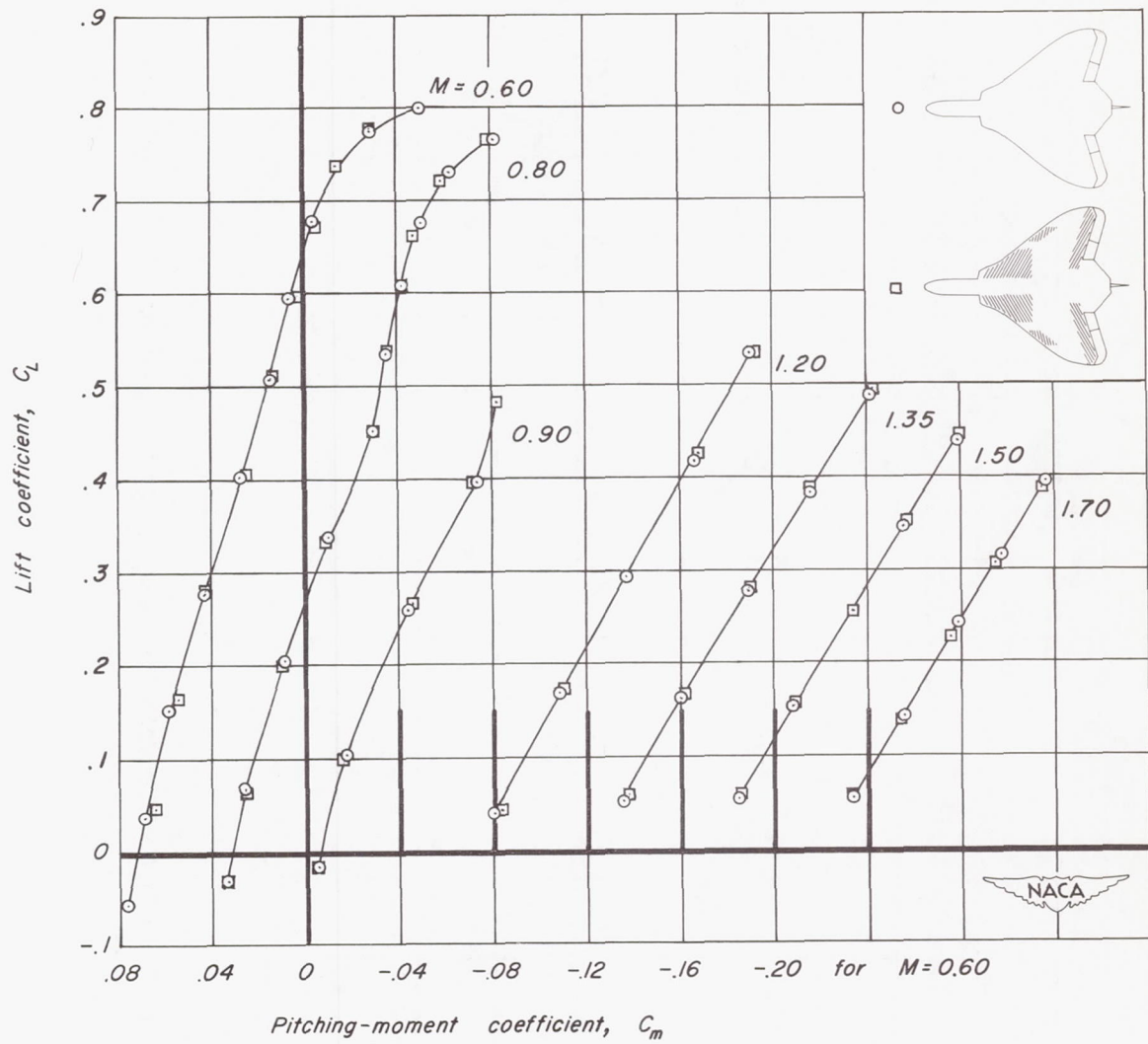
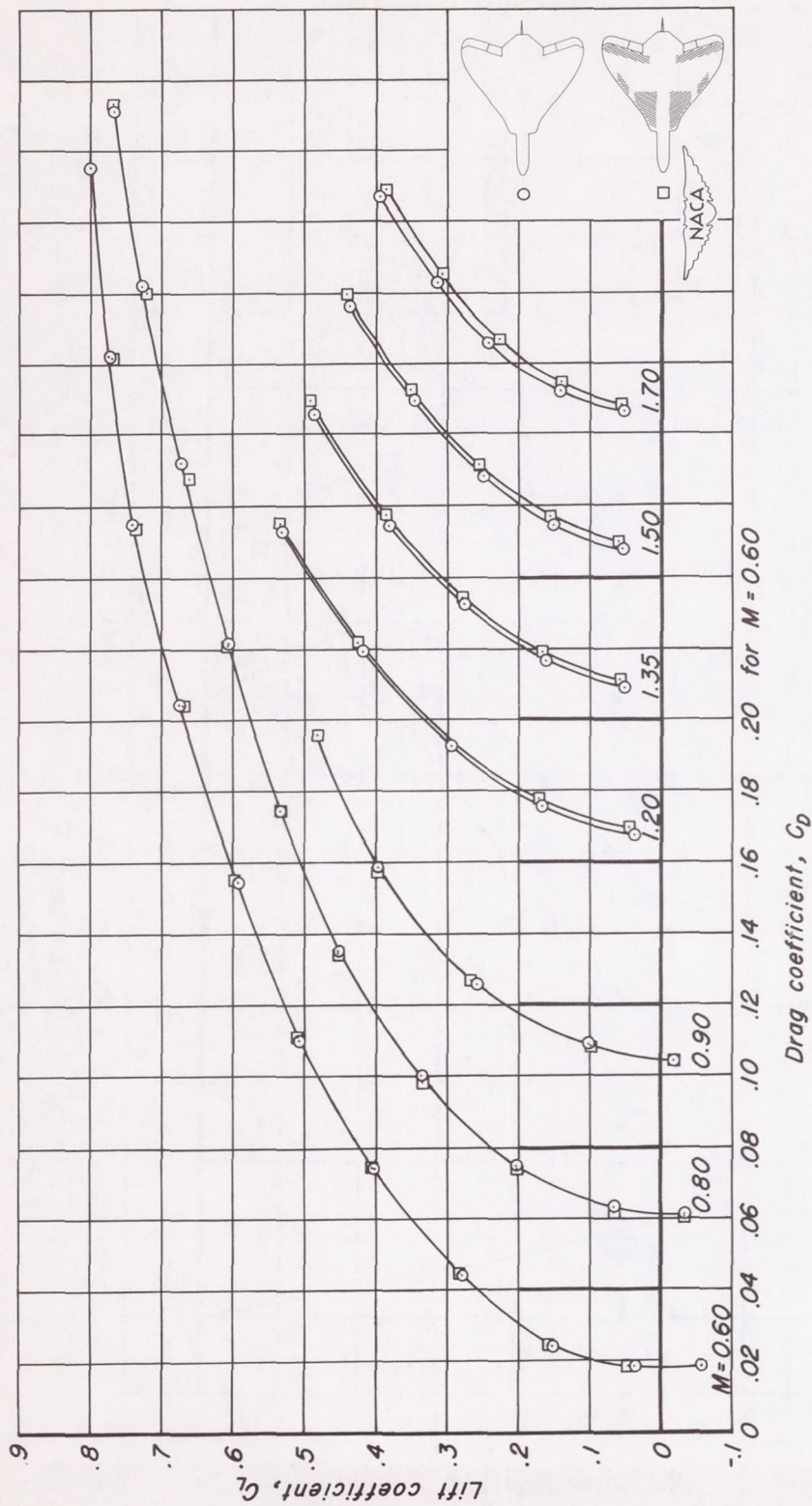
(b)  $C_L$  vs  $C_m$ 

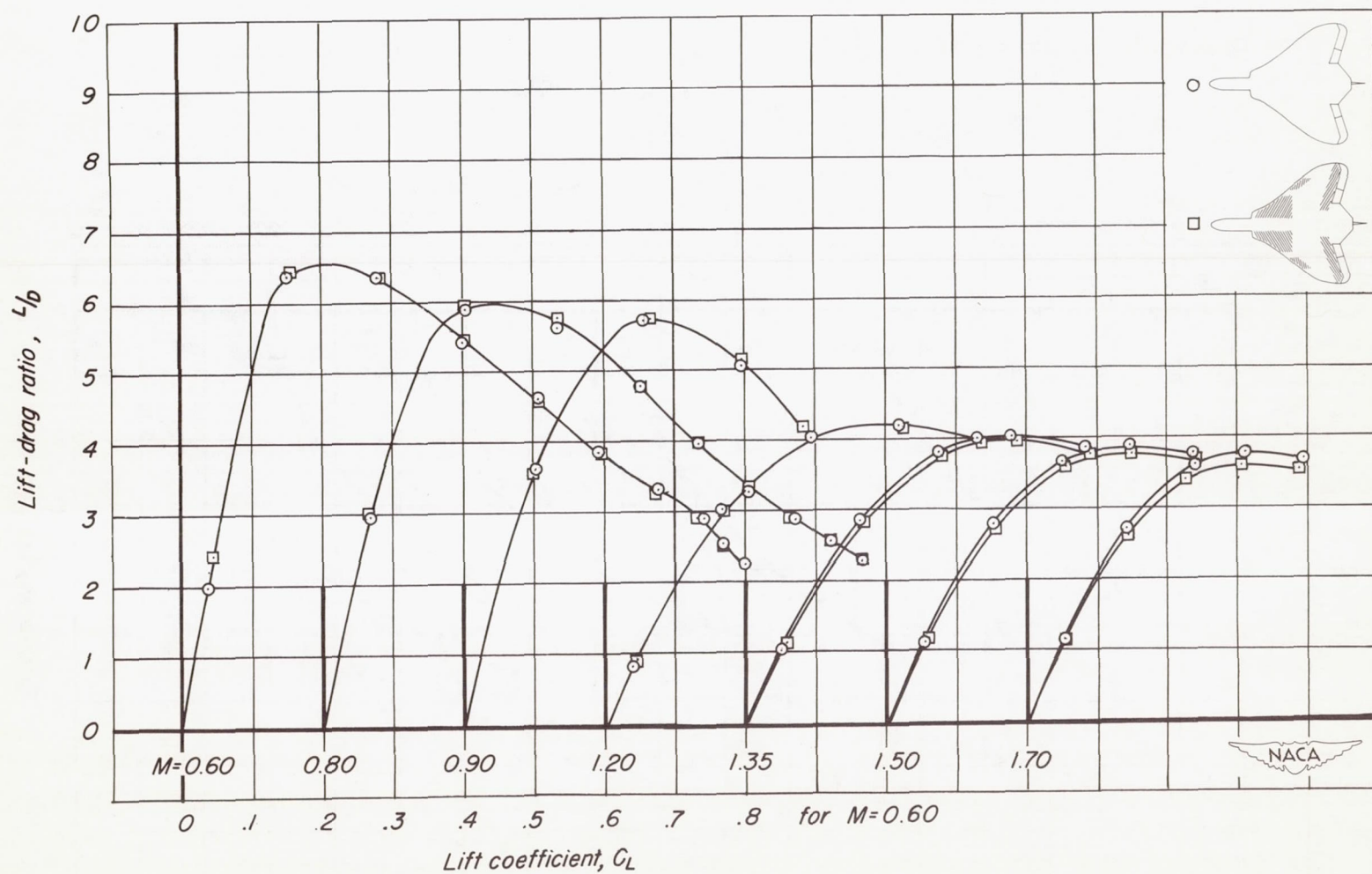
Figure 6.- Continued.



(c)  $C_L$  vs  $C_D$

Figure 6. - Continued.





(d)  $L/D$  vs  $C_L$

Figure 6. - Concluded.

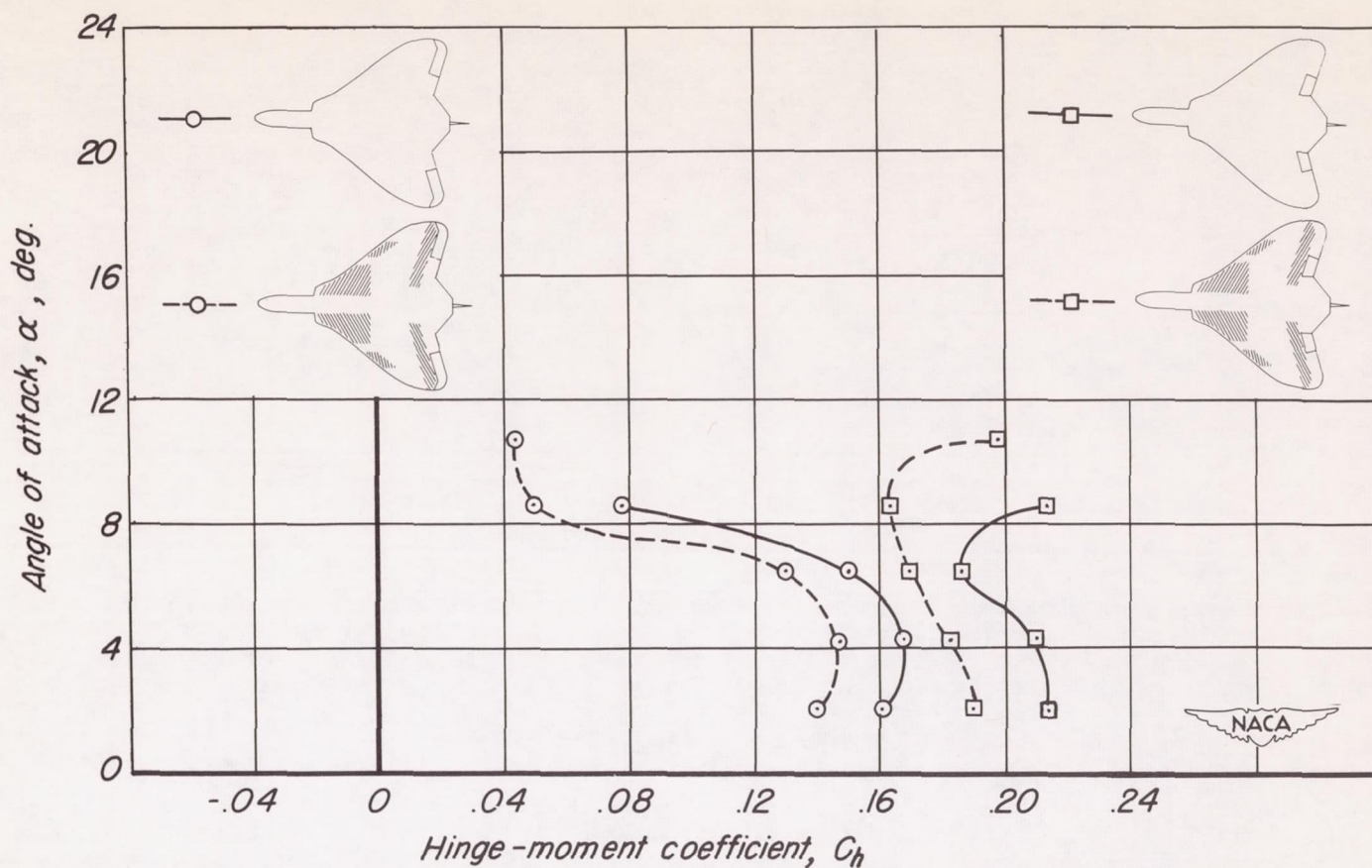


Figure 7.— The effect of simulated skin wrinkles on the hinge-moment characteristics of the inboard elevon and outboard elevon of the swept-wing model. Mach number, 0.90;  $\delta_i, -15^\circ$ ;  $\delta_o, -15^\circ$ .